AKADÉMIAI KIADÓ

Pollack Periodica • An International Journal for Engineering and Information Sciences

19 (2024) 2, 22–29

DOI: 10.1556/606.2024.00888

ORIGINAL RESEARCH PAPER

LMI feasibility analysis of 2DOF NATA model

Andrea Wéber[1]* and Miklós Kuczmann[2]

[1] Doctoral School of Multidisciplinary Engineering Sciences, Széchenyi István University, Győr, Hungary

[2] Department of Power Electronics and Electric Drives, Faculty of Power Electronics and Electric Drives, Széchenyi István University, Győr, Hungary

Received: May 12, 2023 • Revised manuscript received: October 23, 2023 • Accepted: January 9, 2024
Published online: February 19, 2024

ABSTRACT

Present paper shows the different types of tensor product model based linear matrix inequality controller design and feasibility analysis of two degrees of freedom aeroelastic wing section model. The tensor product models are based on reducing or removing the nonlinear behavior of the system and weighting functions. The linear matrix inequality based method results globally asymptotically stable system. The goal of the paper is to examine that selecting and varying the transformation space influences the feasibility of the linear matrix inequality based controller. The paper gives a comparison between the different tensor product models in terms of controller performance. The linear matrix inequality gives feasible solution for the controller design if the transformation space is selected adequately.

KEYWORDS

tensor product transformation, linear matrix inequality, controller performance, reducing non-linearity, feasibility analysis

1. NOTATIONS AND DEFINITIONS

Notations and definitions that used in present paper are

- Indices: $i = 1, 2, \ldots, I$ and $j = 1, 2, \ldots, J$, where I, J are the number of the Linear Time-Invariant system (LTI) vertexes;
- System matrix $\mathbf{S}(p(t))$ is determined with $p = p(\mathrm{t}) \in \Omega$;
- Transformation space $\Omega = [a_1, b_1] \times [a_2, b_2] \times \ldots \times [a_n, b_n] \subset \mathbb{R}^n$, where the Tensor Product (TP) model representation is explainable;
- Weighting functions $w_i = w_i(p(t))$, $w_j = w_j(p(t))$;
- Close to NOrmalised (CNO) type weighting function;
- $\mathbf{x}(t) \in \mathbb{R}^n$ is the state vector, $\mathbf{u}(t) \in \mathbb{R}^m$ is the input vector, $\mathbf{y}(t) \in \mathbb{R}^q$ is the output vector and $\mathbf{A}_i(t) \in \mathbb{R}^{n \times n}$, $\mathbf{B}_i(t) \in \mathbb{R}^{n \times m}$;
- Matrices for Linear Matrix Inequality (LMI), $\mathbf{F}_{i_1,i_2}$ is the controller gain, and $\mathbf{F}_i = \mathbf{M}_i \mathbf{P}_1^{-1}$, $\mathbf{F}_j = \mathbf{M}_j \mathbf{P}_1^{-1}$, where $\mathbf{P}_1 > \mathbf{0}$. Matrices $\mathbf{P}$ and $\mathbf{M}$ can be found by convex optimization methods including LMIs;
- X-type weighting functions: Varying the input space with reduction of non-linearity results less complex weighting functions, (see in Fig. 1) where $w_n(p_n(t))$ are illustrated for n dimensions.

2. INTRODUCTION

Present article shows the different types of TP models of the aeroelastic wing section with LMI based controller design in Parallel Distributed Compensation (PDC) framework via

*Corresponding author.
E-mail: weber.andrea@sze.hu

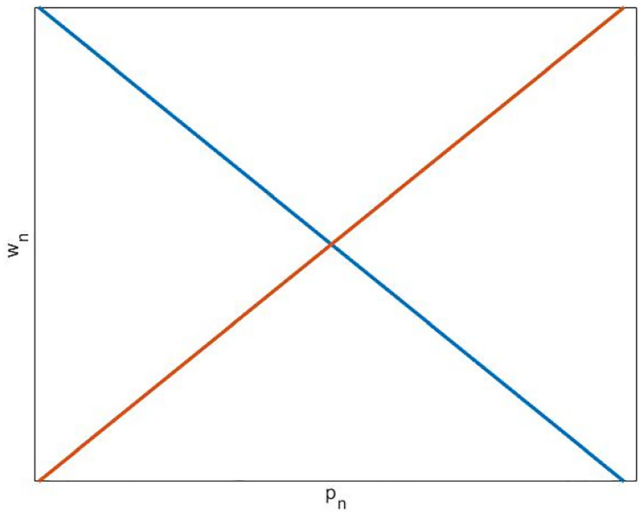

Fig. 1. X-type weighting functions

Higher Order Singular Value Decomposition (HOSVD). The proposed design method results stable controller and the paper proves that it can be selected the better TP model with better control performance. In order to achieve this, it is possible to vary the transformation space and select the parameter space.

Previous paper [1] describes the TP model transformation-based observer and controller design for the same Nonlinear Aeroelastic Test Apparatus (NATA) model. This paper presents that selecting the input space and transformation space has influence on the control performances. In the current paper, the parameters of the wing model, the state-space variables, and the quasi-Linear Parameter Varying (qLPV) state-space representation, the applied parameters and mathematical expressions are the same as in papers [1–3]. The TP transformation is executed on the "original" qLPV model, see in papers [2, 3]. Current paper presents several alternative TP models and shows the LMI feasibility analysis for these models.

Paper [4] proposes the nonlinearity reducing method and changing the number of the inputs for the TP model. The article describes a new type of method to the TP model transformation: how to vary the number of inputs of a given TP model. The paper focuses on how to manipulate the number of inputs of a given Takagi-Sugeno (TS) fuzzy model but also discusses the difference between TS fuzzy and TP models.

The TP model transformation and its extension, LMI and HOSVD based methods are a popular research field today, there are many publications about the investigation; [4–13]. Articles on practical applications of the TP model transformation: [14–24]. Additional papers used for current article: [25, 26].

Current paper presents that varying input space and transformation space has influence on the feasibility regions of LMI. In this paper, the weighting functions are all CNO types, the same grid density is applied for each TP models. Furthermore, if the nonlinearity is reduced, then the feasibility regions of LMI are increased. With these investigations, it can be determined which TP model results better control performance.

3. NOVEL CONTRIBUTION OF THE PAPER

Present paper investigates that reducing non-linearity from the TP models and selecting transformation space influence the design of LMI based controller and the TP model, respectively.

Statement 1. Reducing or removing the nonlinear behavior from the TP models results different TP models and different control performance and the feasibility regions are increased. Selecting the parameter space has influence on the feasibility regions of LMI.
Statement 2. Varying and selecting the transformation space influence the feasibility of the LMI based controller and the TP model. Selection of transformation space shows how the controller changes in LMIs, then it can be chosen the better controller performance. The feasibility test shows that the more the non-linearity decreases, the larger the feasibility region becomes.

Proves. The proves are based on the 2DoF aeroelastic wing section model. The examinations follow these key points:

1. Removing non-linearity from TP models: varying the input space;
2. Applying HOSVD based method in numerical way;
3. HOSVD and TP model transformation generates the LTI vertex systems;
4. LMI feasibility analysis: changing the transformation space;
5. LMI based controller design.

Versions of TP models have different numbers of inputs or combinations of inputs. The key structure for transforming TP models is based on the complexity reduction technique developed in [27], which presents a singular value-based method for reducing a given set of fuzzy rules. The method is able to change the number of inputs and transform the nonlinearity between the fuzzy rules and the input dimensions. These features significantly increase the modeling capability of the TP structure, allowing further complexity reduction and more robust control optimization.

In the present research, the reduction of nonlinearity is achieved by removing nonlinearities: reducing the order of the system and eliminating as much nonlinearity as possible from the system of equations, e.g., $\sin(x_3)$, $\cos(x_3)$, etc. Alternative TP models can be generated from the original TP model, with the advantage that alternative models can have a different number of inputs, or the inputs of the TP model can be specified as a function of the original inputs.

4. TP MODEL VARIANTS OF THE WING SECTION

The mechanical model (Fig. 2) is a two-dimensional typical airfoil in horizontal flow, whose motion is determined by two independent degrees of freedom; vertical displacement (dive) and pitch. The study of the dynamic behaviour of the aeroelastic wing is based primarily on divergence and rudder reversal. The mathematical modeling of the 2DoF aeroelastic wing section model and the parameters are presented in papers [2] and [3].

The state variables of the mechanical model are:

$$\mathbf{x}(t) = \begin{bmatrix} x_1(t) \\ x_2(t) \\ x_3(t) \\ x_4(t) \end{bmatrix} = \begin{bmatrix} h(t) \\ \alpha(t) \\ \dot{h}(t) \\ \dot{\alpha}(t) \end{bmatrix}, \tag{1}$$

where $x_1(t)$ is the plunge displacement and $x_2(t)$ is the pitch displacement. The qLPV state space representation of the model:

$$\dot{\mathbf{x}}(t) = \mathbf{S}(\mathbf{p}(t)) \begin{bmatrix} \mathbf{x}(t) \\ \mathbf{u}(t) \end{bmatrix}, \tag{2}$$

where

$$\mathbf{p}(t) = \begin{bmatrix} U(t) \\ x_2(t) \end{bmatrix}, \tag{3}$$

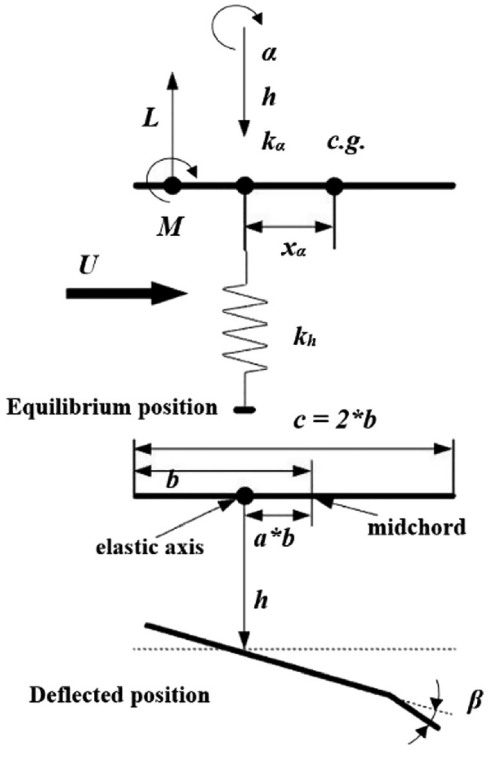

Fig. 2. Two-dimensional airfoil plate

where $U(t)$ is the free stream velocity and the system matrix is as follow:

$$\mathbf{S}(\mathbf{p}(t)) = [\,\mathbf{S}_1(\mathbf{p}(t)) \quad \mathbf{S}_2(\mathbf{p}(t))\,], \tag{4}$$

$$\mathbf{S}_1(\mathbf{p}(t)) = \begin{bmatrix} 0 & 0 \\ 0 & 0 \\ -k_1 & -k_2U^2(t) - p(k_\alpha(x_2(t))) \\ -k_3 & -k_4U^2(t) - q(k_\alpha(x_2(t))) \end{bmatrix}, \tag{5}$$

$$\mathbf{S}_2(\mathbf{p}(t)) = \begin{bmatrix} 1 & 0 & 0 \\ 0 & 1 & 0 \\ -c_1(U(t)) & -c_2(U(t)) & g_3U^2(t) \\ -c_3(U(t)) & -c_4(U(t)) & g_4U^2(t) \end{bmatrix}, \tag{6}$$

where the mathematical expressions and parameters are described in papers [2] and [3].

4.1. TP model 1

This model is the "original" TP model, where the parameters are not changed [2–4]. The weighting functions are CNO types for all TP models. After using HOSVD method on the system matrix (4), the following TP model transformation describes the nonlinear model:

$$\dot{\mathbf{x}} \cong \sum_{i=1}^{3} \sum_{j=1}^{2} w_i(U) w_j(x_2) \left(\mathbf{A}_{i,j}\mathbf{x} + \mathbf{B}_{i,j}\mathbf{u}\right), \tag{7}$$

where

$$\mathbf{u} = -\left(\sum_{i=1}^{3} \sum_{j=1}^{2} w_i(x_1) w_j(x_2) \mathbf{F}_{i,j}\right)\mathbf{x}. \tag{8}$$

Therefore the number of LTI vertex models are $3\times2 = 6$. Here, the parameters are $p_1(t) = U(t)$, $p_2(t) = x_2(t)$ and the transformation space $\Omega = [14, 25]\times[-0.3, 0.3]$ with grid density 137. The weighting functions of TP model 1 are shown in Fig. 3. It can be seen that there are $w_{1,1}, w_{1,2}, w_{1,3}$ weighting functions for p_1, and $w_{2,1}, w_{2,2}$ weighting functions for p_2. The next step is to remove or reduce the nonlinear behavior of the TP model 1.

4.2. TP model 2

To reduce the nonlinearity, new parameter space is introduced: $p_1(t) = U(t)$ and $p_2(t) = k_\alpha(x_2(t))$. The transformation space is the same, as in case of the TP model 1. Here, the generated LTI vertex systems are $3\times2 = 6$:

$$\dot{\mathbf{x}} \cong \sum_{i=1}^{3} \sum_{j=1}^{2} w_i(U) w_j(k_\alpha(x_2)) \left(\mathbf{A}_{i,j}\mathbf{x} + \mathbf{B}_{i,j}\mathbf{u}\right). \tag{9}$$

Figure 4 shows that $w_{1,1}$, $w_{1,2}$, $w_{1,3}$ weighting functions of parameter $p_1(t)$ are the same as in case of TP model 1. $x_2(t)$ has influence on the system matrix. $w_{2,1}$, $w_{2,2}$ are X-type weighting functions for $p_2(t)$.

The nonlinear behavior of the weighting functions are removed in the second dimension, therefore the dimension of $x_2(t)$ has changed. It can be noticed that the complexity of the second dimension is decreased compared to the first TP model.

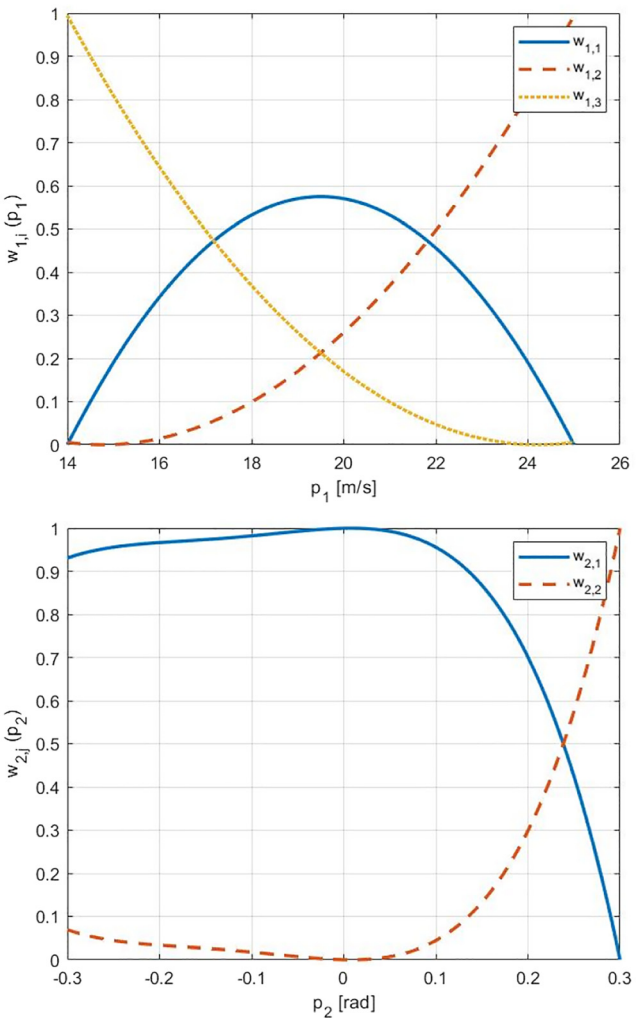

Fig. 3. Weighting functions of TP model 1

4.3. TP model 3

Here, a new parameter is introduced: $p_2(t) = U^2(t)$, so the parameter space now is $p_1(t) = U(t)$, $p_2(t) = U^2(t)$, $p_3(t) = x_2(t)$ and the transformation space $\Omega = [14, 25] \times [14^2, 25^2] \times [-0.3, 0.3]$. After executing HOSVD, there are $2 \times 2 \times 2 = 8$ LTI vertex systems. The structure of the TP model transformation is as follow:

$$\dot{\mathbf{x}} \cong \sum_{i=1}^{2} \sum_{j=1}^{2} \sum_{k=1}^{2} w_i(U) w_j\left(U^2\right) w_k(x_2) \left(\mathbf{A}_{i,j,k}\mathbf{x} + \mathbf{B}_{i,j,k}\mathbf{u}\right). \tag{10}$$

The weighting functions $w_{1,1}$, $w_{1,2}$ and $w_{2,1}$, $w_{2,2}$ are X-type for parameters $p_1(t)$ and $p_2(t)$. For $p_3(t)$, $w_{3,1}$, $w_{3,2}$ functions are illustrated in Fig. 5. In the first two dimensions, the weighting functions are less complex and there is a new dimension but the maximum number of the weighting functions are two. The number of the LTI systems are increased but reducing the nonlinear behavior is still possible.

4.4. TP model 4

This TP model is the combination of TP model 2 and 3. The parameters are $p_1(t) = U(t)$, $p_2(t) = U^2(t)$ and $p_3(t) = k_\alpha(x_2(t))$, the transformation space is $\Omega = [14, 25] \times [14^2, 25^2] \times [-0.3, 0.3]$. Here, the number of the LTI system are $2 \times 2 \times 2 = 8$:

$$\dot{\mathbf{x}} \cong \sum_{i=1}^{2} \sum_{j=1}^{2} \sum_{k=1}^{2} w_i(U) w_j\left(U^2\right) w_k(k_\alpha(x_2)) \left(\mathbf{A}_{i,j,k}\mathbf{x} + \mathbf{B}_{i,j,k}\mathbf{u}\right). \tag{11}$$

The weighting functions $w_{1,1}$, $w_{1,2}$, $w_{2,1}$, $w_{2,2}$ and $w_{3,1}$, $w_{3,2}$ are all X-types. Therefore, it can be seen that the maximum number of the functions are two and this model is more simpler than the previous three TP models.

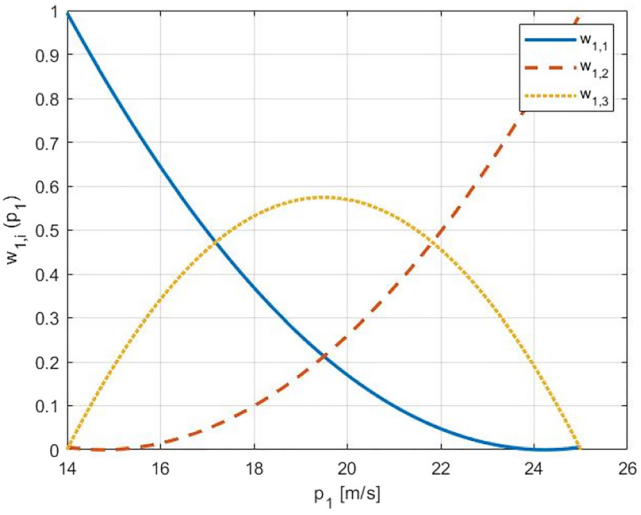

Fig. 4. Weighting functions of TP model 2

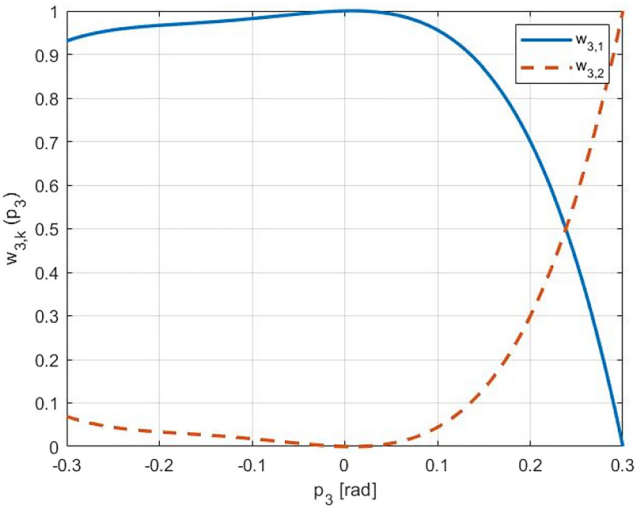

Fig. 5. Weighting functions of TP model 3

5. LMI FEASIBILITY ANALYSIS

Changing the transformation space Ω has influence on the LMI feasibility regions. Therefore the analysis of the feasibility test shows whether or not exist solution for LMIs. Consider the following solver for LMI feasibleness problems $\mathbf{L}(x)<\mathbf{R}(x)$, where $\mathbf{R}$ is the feasibility radius. The solver is minimizes t subject to $\mathbf{L}(x)<\mathbf{R}(x)+t\mathbf{I}$. Therefore, t should be negative for feasible solution.

The analysis only includes the change of the transformation space in one dimension, i.e., the transformation space is not changed in several dimensions at the same time.

In the figures, x-axis shows p_{min}, y-axis shows p_{max} parameters. In the illustrations, it is presented that the LMI can be solved in the given interval in different dimensions. Thus, the regions marked with black dots are the feasible regions and the regions marked with empty circles are the non-feasible regions.

5.1. LMI feasibility regions of TP model 1

Figure 6 illustrates the LMI feasibility regions of the TP model 1. In the first case the transformation space is changed in the first dimension for parameter $p_1(t)$ and fixed in the second dimension on interval $[-,-]\times[-0.3,0.3]$. The figures presents the regions of the LMI feasibility from $U=[1,5]$ to $U=[40,534]$. The second case shows extending of the transformation space $\Omega=[14,25]\times[-,-]$ for parameter $p_2(t)$.

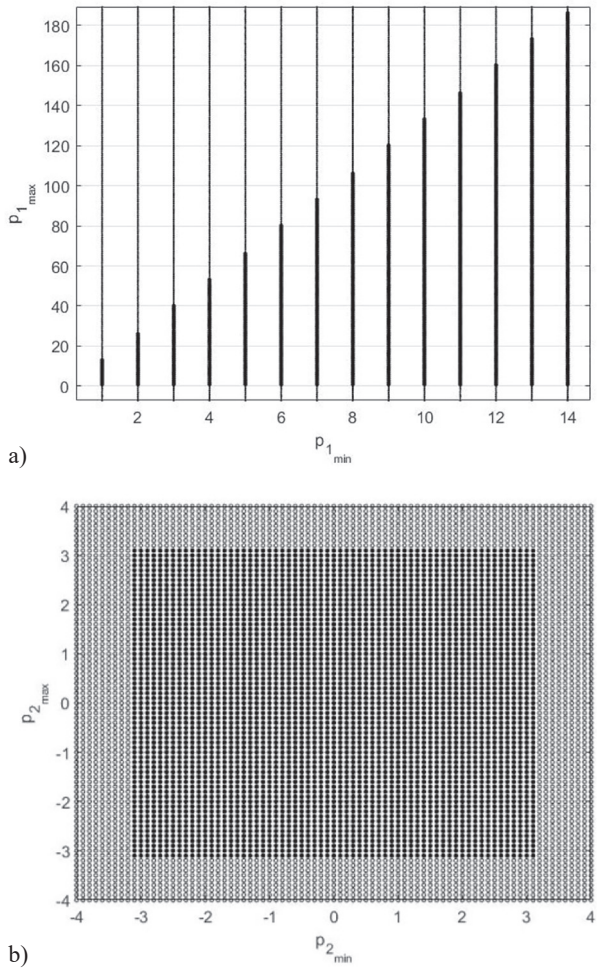

Fig. 6. LMI feasibility regions of TP model 1, a) first case, b) second case

5.2. LMI feasibility regions of TP model 2

The LMI feasibility regions of TP model 2 are the same as the previous model (Fig. 6) on the examined interval. It can be seen that the transformation space is changed in the first dimension related to $p_1(t)$ on interval $[-,-]\times[-0.3,0.3]$. In the second case, the second dimension is changed on interval $[14,25]\times[-,-]$ for parameter $p_2(t)$. The figures show that the feasibility regions are the same within the interval considered, but the nonlinearity was removed. Feasibility growth occurs outside the examined interval.

5.3. LMI feasibility regions of TP model 3

Here, changing the transformation space is illustrated in Fig. 7. It can be seen that the first dimension is modified for $p_1(t)=U(t)$ and the others are fixed on interval $[-,-]\times[14^2,25^2]\times[-0.3,0.3]$. Then, the third dimension is changed and the first and second dimensions are fixed on interval $[14,25]\times[14^2,25^2]\times[-,-]$ for $p_3(t)$. It can be noticed that the LMI feasibility region is increased for parameter $p_1(t)$ compared to previous TP models.

5.4. LMI feasibility regions of TP model 4

The LMI feasibility analysis shows that the LMI based controller is feasible and regions and given intervals are the same as TP model 3, see in Fig. 7, but feasibility regions can occur outside the examined interval. The first case illustrates when the transformation space is changed in the first interval and the second and third intervals are fixed on $[-,-]\times[14^2,25^2]\times[-0.3,0.3]$. The second case shows that the third dimension is changed in transformation space $[14,25]\times[14^2,25^2]\times[-,-]$ for parameter $p_3(t)$. Consequently, this TP model covers larger LMI feasibility regions.

In summary, as the nonlinear property is gradually reduced, the LMI feasibility region increases, which can be proved by varying and extending the transformation space Ω.

6. STABLE CONTROLLER DESIGN

The method of LMI allows the stability of the system to be achieved if LMI is feasible for different TP models. The polytopic model with controller is asymptotically stable if there exist such positive definite matrices $\mathbf{X}>0$ and $\mathbf{M}_i$ satisfies the following conditions:

$$-\mathbf{X}\mathbf{A}_i^T-\mathbf{A}_i\mathbf{X}+\mathbf{M}_i^T\mathbf{B}_i^T+\mathbf{B}_i\mathbf{M}_i\succ\mathbf{0}, \tag{12}$$

for all i,

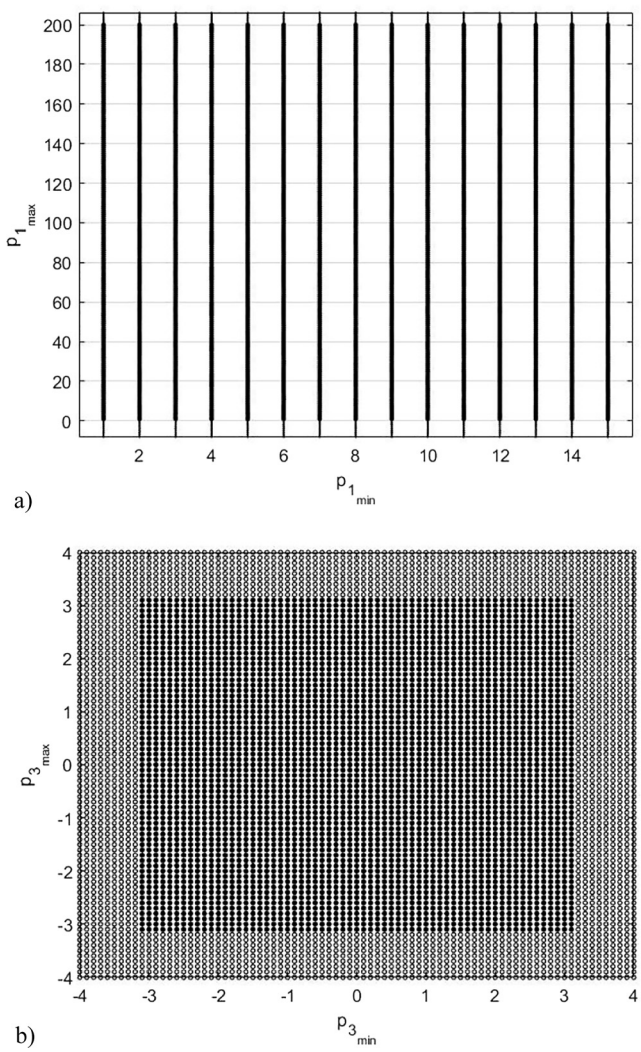

Fig. 7. LMI feasibility regions of TP model 3, a) first case, b) second case

$$-\mathbf{X}\mathbf{A}_i^T - \mathbf{A}_i\mathbf{X} - \mathbf{X}\mathbf{A}_j^T - \mathbf{A}_j\mathbf{X} + \mathbf{M}_j^T\mathbf{B}_i^T + \mathbf{B}_i\mathbf{M}_j + \mathbf{M}_i^T\mathbf{B}_j^T + \mathbf{B}_j\mathbf{M}_i \geq 0, \tag{13}$$

for all $i<j \leq I$ and $\forall \mathbf{p}(t) : w_i(\mathbf{p}(t))t))\mathbf{p}w_j(\mathbf{p}(t)) = 0$, where $i = 1, \cdots, I$, $j = i + 1, \cdots, I$ and I is the number of the LTI systems, from the feedback gain solutions $\mathbf{X}$ and $\mathbf{M}_i$: $\boldsymbol{F}_i = \boldsymbol{M}_i\boldsymbol{X}^{-1}$.

The initial conditions for all TP models are $[h, \alpha, \dot{h}, \dot{\alpha}]^T = [0.01, 0.1, 0, 0]^T$. Figure 8 shows the x_1 and x_2 state variables i.e., plunge displacement h and pitch displacment α, the u control signal of the wing section model. These figures also show the different TP models with reduced non-linearity. Therefore, TP models give different results for the LMI based controller in terms of stability. The present TP models are investigated based on the objective to reduce the oscillation rate for each model and to reach the steady state sooner.

It can be seen in case of state variables x_1, the steady state is reached in about 0.4 to 0.8 seconds. The oscillation rate is

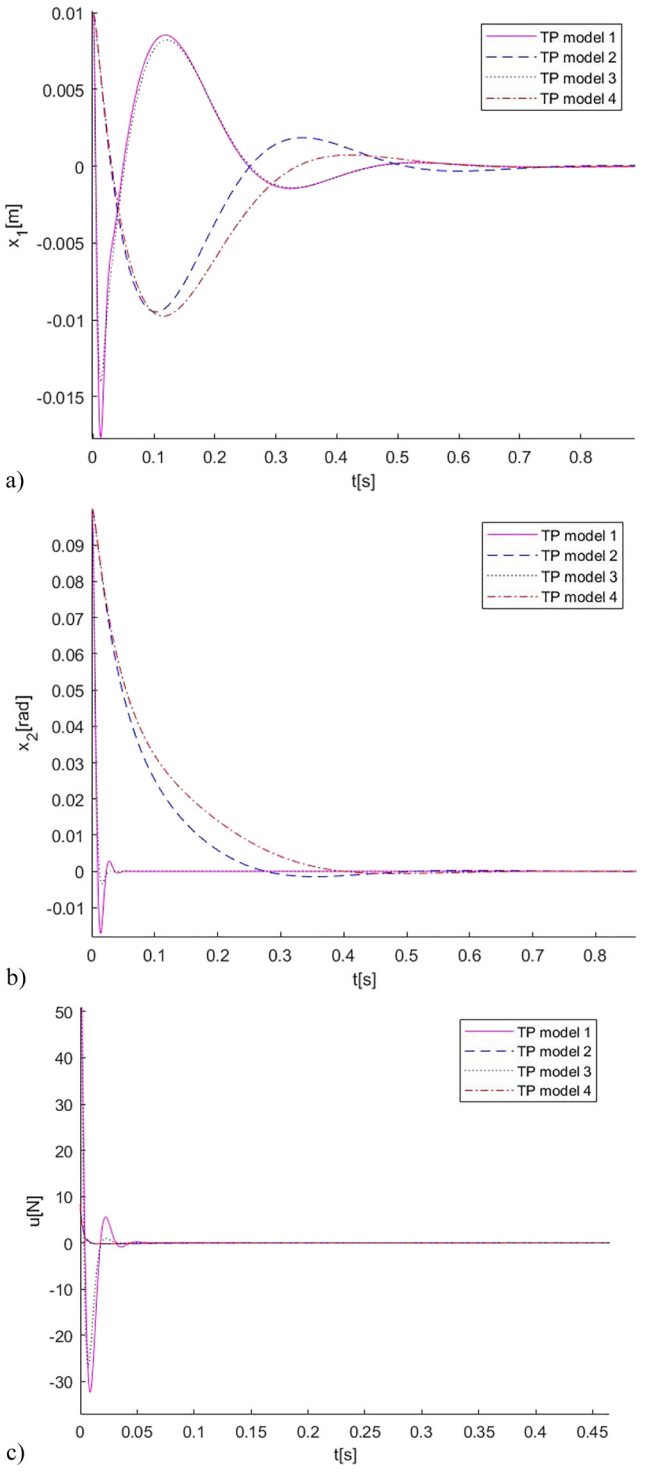

Fig. 8. State variables and control signals for all TP models, a) state variable x_1; b) state variable x_2; c) control signal u

highest between 0 and 0.3 seconds. The purple colour indicates the state variable x_1 of TP model 1, i.e. the "original system". It can be noticed that the oscillations are larger for TP models 1 and 3. The figure shows that TP model 4 stabilizes faster and has smaller oscillation magnitude.

Furthermore, Fig. 8 shows that in case of state variables x_2, the system stabilizes faster between about 0 and 0.1

seconds forTP models 1 and 3, but for TP models 2, 4, the function decays faster and the system reaches steady state faster because there is less oscillation. For the latter two models, stabilisation occurs between about 0.4 and 0.8 seconds. It is clear that TP model 3 performs better for state variable x_2.

Finally, the control signal u showed in Fig. 8, that illustrates that TP model 2 has better control performance. In case of TP model 1 and 3, the control signals have lower controller performance because the system takes longer to reach steady state.

7. CONCLUSION

Current paper presents the TP transformation based controller design of 2DoF aeroelastic wing section through HOSVD method in PDC framework. The controller is designed for each TP models and the controllers are accomplished with LMI based method. The paper gives a comparison between the TP models with different nonlinearity via choosing parameter space and varying transformation spaces. Consequently, it can be noted that selecting transformation space and input space results different control performance. The LMI feasibility test shows that the smaller the nonlinearity, the larger the feasibility region of the TP models. Then, we can choose the better TP model with better control performance. As a result, the TP model 4 is the simpler model from point of reducing nonlinearity and the controller performance.

REFERENCES

[1] A. Wéber and M. Kuczmann, "TP transformation based observer and controller design of 2DoF aeroelastic wing section model," in *1st International Conference on Internet of Digital Reality*, Gyor, Hungary, June 23–24, 2022, pp. 000017–000022.

[2] P. Baranyi, "Output feedback control of two-dimensional aeroelastic system," *J. Guidance, Control Dyn.*, vol. 29, no. 3, pp. 762–766, 2006.

[3] P. Baranyi, "Tensor-product model-based control of two-dimensional aeroelastic system," *J. Guidance, Control Dyn.*, vol. 29, no. 2, pp. 391–400, 2006.

[4] P. Baranyi, "How to vary the input space of a TS fuzzy model: a TP model transformation based approach," *IEEE Trans. Fuzzy Syst.*, vol. 30, no. 2, pp. 345–356, 2020.

[5] P. Baranyi, Y. Yam, and P. Várlaki, *Tensor Product Model Transformation in Polytopic Model Based Control.* 1st ed., CRC Press, Taylor and Francis Group, 2018.

[6] G. Bergqvist and E. Larsson, "The higher order singular value decomposition: Theory and an application," *IEEE Signal Process. Mag.,* vol. 27 no. 3, pp. 151–154, 2010.

[7] P. Szeidl and P. Várlaki, "HOSVD based canonical form for polytopic models of dynamic systems," *J. Adv. Comput. Intelligence Intell. Inform.*, vol. 13, no. 1, pp. 52–60, 2009.

[8] K. Tanaka and H. O. Wang, "Fuzzy regulators and fuzzy observers: a linear matrix inequality approach," in *Proceedings of the 36th IEEE Conference on Decision and Control*, San Diego, CA, USA, December 12-12, 1997, pp. 1315–1320.

[9] D. Tikk, P. Baranyi, and R. Patton, "Approximation properties of TP model forms and its consequences to TPDC design framework," *Asian J. Control*, vol. 9, no. 3, pp. 221–231, 2007.

[10] P. Korondi, "Tensor product model transformation-based sliding surface design," *Acta Polytech. Hungarica*, vol. 3, no. 4, pp. 23–35, 2006.

[11] Y. Yam, "Fuzzy approximation via grid point sampling and singular value decomposition," *IEEE Trans. Syst. Man, Cybernetics*, Part B, vol. 27, no. 6, pp. 933–951, 1997.

[12] X. Liu, X. Xin, Z. Li, and Z. Chen, "Near optimal control based on the tensor-product technique," *IEEE Trans. Circuits Syst. Express Briefs*, vol. 64, no. 5, pp. 560–564, 2017.

[13] K. Tanaka and H. O. Wang, *Fuzzy Control Systems Design and Analysis: A Linear Matrix Inequality Approach.* John Wiley and Sons, 2001.

[14] A. Szollosi and P. Baranyi, "Influence of the tensor product model representation of qLPV models on the feasibility of linear matrix inequality," *Asian J. Control,* vol. 18, no. 4, pp. 1328–1342, 2016.

[15] A. Wéber and M. Kuczmann, "TP transformation based controller and observer design of the inverted pendulum," *Przeglad Elektrotechniczny*, vol. 98, no. 10, pp. 34–39, 2022.

[16] A. Wéber and M. Kuczmann, "TP transformation of the inverted pendulum," in *2nd IEEE International Conference on Gridding and Polytope Based Modeling and Control*, Gyor, Hungary, November 19-19, 2020, pp. 13–18, 2020.

[17] M. Kuczmann, "Study of tensor product model alternatives," *Asian J. Control*, vol. 23, no. 3, pp. 1249–1261, 2021.

[18] A. Szollosi and P. Baranyi, "Influence of the tensor product model representation of qLPV models on the feasibility of linear matrix-based stability analysis," *Asian J. Control,* vol. 20, no. 1, pp. 531–547, 2018.

[19] B. Takarics, A. Szollosi, and B. Vanek, "Tensor product type polytopic LPV modeling of aeroelastic aircraft," in *2018 IEEE Aerospace Conference*, Big Sky, MT, USA, March 3-10, 2018, pages 1–10.

[20] J. Ko, A. J. Kurdila, and T. W. Strganac, "Nonlinear control of a prototypical wing section with torsional nonlinearity," *J. Guidance, Control Dyn.*, vol. 20, no. 6, pp. 1181–1189, 1997.

[21] J. Kuti, P. Galambos, and A. Miklós, "Output feedback control of ´ a dual-excenter vibration actuator via qLPV model and TP model transformation," *Asian J. Control*, vol. 17, no. 2, pp. 432–442, 2015.

[22] B. Takarics and P. Baranyi, "Tensor-product-model-based control of a three degrees- of-freedom aeroelastic model," *J. Guidance, Control Dyn.*, vol. 36, no. 5, pp. 1527–1533, 2013.

[23] A. M. F. Pereira, L. M. S. Vianna, N. A. Keles, and V. C. da Silva Campos, "Tensor product model transformation simplification of Takagi-sugeno control and estimation laws–an application to a thermoelectric controlled chamber," *Acta Polytech. Hungarica*, vol. 15, no. 3, pp. 13–29, 2018.

[24] A. Boonyaprapasorn, S. Kuntanapreeda, T. Sangpet, P. S. Ngiamsunthorn, and E. Pengwang, "Biological pest control based

on tensor product transformation method," *Acta Polytech. Hungarica*, vol. 17, no. 6, pp. 25–40, 2020.

[25] Z. Németh and M. Kuczmann, "State space modeling theory of induction machines," *Pollack Period.*, vol. 15, no. 1, pp. 124–135, 2020.

[26] F. Hajdu, "Numerical examination of nonlinear oscillators," *Pollack Period.*, vol. 13, no. 3, pp. 95–106, 2018.

[27] Y. Yam, P. Baranyi, and C. T. Yang, "Reduction of fuzzy rule base via singular value decomposition," *IEEE Trans. Fuzzy Syst.*, vol. 7, no. 2, pp. 120–132, 1999.